Published in final edited form as:
Annu Rev Phys Chem. 2007 ; 58: 299–320. doi:10.1146/annurev.physchem.58.032806.104657.

Copper and the Prion Protein: Methods, Structures, Function, and Disease

Glenn L. Millhauser
Department of Chemistry and Biochemistry, University of California, Santa Cruz, California 95064

Glenn L. Millhauser: glennm@chemistry.ucsc.edu

Abstract

The transmissible spongiform encephalopathies (TSEs) arise from conversion of the membrane-bound prion protein from PrP^{C} to PrP^{Sc}. Examples of the TSEs include mad cow disease, chronic wasting disease in deer and elk, scrapie in goats and sheep, and kuru and Creutzfeldt-Jakob disease in humans. Although the precise function of PrP^{C} in healthy tissues is not known, recent research demonstrates that it binds Cu(II) in an unusual and highly conserved region of the protein termed the octarepeat domain. This review describes recent connections between copper and PrP^{C}, with an emphasis on the electron paramagnetic resonance elucidation of the specific copper-binding sites, insights into PrP^{C} function, and emerging connections between copper and prion disease.

Keywords

transmissible spongiform encephalopathies; electron paramagnetic resonance; octarepeat domain; neuroprotection; apoptosis

Introduction

Prion diseases result from the accumulation of a misfolded form of the endogenous prion protein (PrP) and present an ongoing threat to human health, and agricultural and wildlife animals (1–5). Referred to as the transmissible spongiform encephalopathies (TSEs), these fatal, neurodegenerative diseases share pathologies with Alzheimer's and Parkinson's disease (6). What sets the TSEs apart, however, is that the misfolded prion protein is an infectious agent. As such, single instances of mad cow disease (bovine spongiform encephalopathy) create immediate concern with regard to the safety of our food supply and greatly affect the cattle industry (7). Chronic wasting disease has infected upward of 15% of deer and elk in the U.S. and Canadian Rocky Mountain regions (8). Although prion diseases in humans are rare, those cases in which transmission has taken place certainly motivate extreme caution. Approximately 140 young individuals in the United Kingdom have died from variant Creutzfeldt-Jakob disease (vCJD) contracted from bovine spongiform encephalopathy–contaminated food (9,10). Surgical procedures involving corneal transplants and dura mater grafts have transmitted disease to healthy individuals, as have contaminated surgical instruments and cadaver-derived hormones (5). At this time, it is unknown whether blood transfusions are able to transmit prion diseases (11).

PrP is a membrane-bound glycoprotein found in the central nervous system (CNS) of all mammals and avian species (3,5,12). Post-translational modification removes the first 22 residues to give mature PrP(23–231). The protein is tethered to the outside surface of cellular membranes by a glycosylphosphatidylinositol anchor at its C terminus (Figure 1). The normal cellular form is designated PrP^{C}. The pathogenic form (the prion), responsible for the TSEs, is designated PrP^{Sc} (scrapie form) and differs from PrP^{C} only in conformation (2,3). Nuclear

magnetic resonance (NMR) studies on recombinant human PrP^C demonstrate that the C-terminal region, starting at approximately residue 125, adopts a globular fold that is largely helical, but with a small two-strand β-sheet (13). Similar structures are found for hamster and mouse PrP^C (14–16). There are currently no high-resolution structures for PrP^{Sc}, but recent electron-crystallography experiments suggest that residues 89–175 refold into a β-helix (17, 18).

PrP's N-terminal region, up to approximately residue 110,is unstructured and flexible in solution (19). A hallmark of this region is the so-called octarepeat domain composed of tandem repeats of the fundamental eight-residue sequence PHGGGWGQ (Figure 1). Most species, including humans, have four or five repeat segments. Interestingly, the octarepeat domain is among the most highly conserved regions of the prion protein (20).

Prion diseases, the TSEs, may be sporadic, inherited, or infectious (21). Sporadic disease, in which PrP^C spontaneously misfolds to PrP^{Sc}, is by far the most common, accounting for roughly 85% of cases in humans (21). Inherited diseases typically arise from mutations in the C-terminal domain (2); by contrast, polymorphisms or mutations in the octarepeat domain are rare (20). Sporadic and inherited prion diseases fall into the same class as Alzheimer's and Parkinson's disease insofar that all are associated with the accumulation of endogenous protein aggregates (21). As noted above, what sets prion diseases apart is that they are infectious. The passage of brain material from diseased animals (mice, hamsters, primates) into healthy animals causes the symptoms of the TSEs, along with the associated buildup of infectious PrP^{Sc} (2,5). Treatment of brain-derived inoculants with radiation or other means of destroying nucleic acids fails to reduce the prion titer (3). Conversely, treatment with certain protein denaturants fully inactivates PrP^{Sc} (22). These unusual findings motivate the protein-only prion hypothesis, which posits that PrP alone, in the form of PrP^{Sc}, constitutes the infectious prion particle (5,21). Researchers have now demonstrated that under partially denaturing conditions, amyloid fibrils generated from recombinant-mouse PrP indeed produce infectious material, the so-called synthetic prions (23).

The specific function of PrP^C in healthy tissues is unknown—determining this function represents one of the great challenges in prion biology. Interestingly, the functions of the proteins responsible for Parkinson's disease and the extracellular deposits in Alzheimer's disease are also unknown. However, within the past several years, it has become clear that the prion protein binds copper in vivo, and the interaction between PrP^C and copper requires the highly conserved, N-terminal octarepeat domain (24–29). Brown et al. (24) report that brain extracts from PrP-knockout mice have lower copper content than wild type, and they also exhibit reduced copper-metalloprotein activity. PrP^C is constitutively cycled from the cell surface to the interior through endocytosis. The addition of Cu^{2+} rapidly stimulates this process, resulting in significant PrP^C internalization (30). Neurons in cell culture are able to sequester Cu^{2+} at the plasma membrane in concentrations dictated by the level of PrP^C expression (31). The PrP octarepeats are highly selective for Cu^{2+}, with affinity for Cu^+ or other metal-ion species either weak or nonexistent (27,29,32).

Within the CNS, PrP^C is concentrated at presynaptic membranes (33), where neurotransmitter release drives communication between neurons. Interestingly, the presynaptic membrane is also a region of high copper localization and flux (34–36). Copper moves from the cell interior to the synaptic space through both exocytosis and neuronal depolarization. Copper efflux may be an obligatory event associated with vesicle fusion, leading to neurotransmitter release (37). There are ongoing experiments to determine exact copper concentrations at the synapse. The best measurements place the resting concentration at approximately 1.0 μM and peak concentrations between 3.0 μM and 250 μM (35,36).

Several lines of investigation have firmly established that PrP^C helps maintain the integrity of neurons (i.e., the protein acts as a neuroprotectant). Compared with PrP knockouts, wild-type nerve cells in culture are much more resistant to deleterious oxidative chemistry mediated by copper or reactive oxygen species; this resistance requires the octarepeat domain (38). Transgenic mice lacking PrP, as they age, present widespread tissue damage, mainly through protein and lipid oxidation (39).

The findings discussed above and numerous other studies show that PrP^C selectively binds copper, and this interaction is required for neuroprotective function. So what is the precise function of PrP^C? There are a number of intriguing possibilities and a good bit of controversy. One prominent idea advanced by Brown and colleagues (40) is that PrP^C is a neuronal superoxide dismutase (SOD) that converts O_2^- to peroxide and oxygen. Despite the attractiveness of this proposal, other labs have failed to demonstrate SOD activity (41,42). Another possibility is that PrP^C endocytosis transports copper from the extracellular space to the cell interior (29–31,43,44). However, measurements of copper transport do not show any dependence on PrP expression levels. PrP^C is also implicated in copper buffering (32), copper sensing (37), signal transduction (45), the suppression of apoptosis (46), copper-reductase activity (47), and neuron development (48).

Elucidating the structural features of the copper centers in PrP is clearly essential for fleshing out function and for testing hypotheses related to neuroprotection. Although X-ray crystallography and NMR are the canonical approaches for determining protein structures, each method encounters challenges when applied to the copper-occupied, full-length prion protein. PrP has proven difficult to crystallize and, to date, only two PrP X-ray structures have been reported, both of the ovine C-terminal domains (49,50). High-resolution NMR, conversely, is confounded by the presence of paramagnetic Cu^{2+}, which leads to significant line broadening. To investigate structural features of the PrP copper sites, our laboratory applies a wide range of electron paramagnetic resonance (EPR) techniques, in conjunction with recombinant PrP and designed peptides. In the sections below, I review the basic EPR methodologies, newly identified PrP structural features, the affinity and cooperativity of copper binding, potential functions of the cellular prion protein, and possible connections between copper and the TSEs.

Electron Paramagnetic Resonance Methodologies

PrP takes up Cu^{2+}, the dominant form of exchangeable copper in the extracellular space. Cu^{2+} is a d^9 transition-metal center with a single unpaired electron. The two naturally occurring isotopes of copper, ^{63}Cu and ^{65}Cu, have $I=\frac{3}{2}$ nuclear spins, so each isotopic species gives rise to nearly equivalent four hyperfine line EPR spectra. As demonstrated many years ago by Peisach & Blumberg (51), both the *g*-tensor and hyperfine tensor (*A*) are sensitive to the equatorial-coordination environment. Analysis of the $g_\parallel$ and $A_\parallel$ features, usually derived from low-temperature spectra (77 K), provides an estimate of the number of coordinating nitrogen and oxygen atoms and the overall charge of the copper center. Moreover, examination of the parallel region often reveals whether there is more than one type of coordination environment and if pH or other factors influence the various coordination modes.

For example, Figure 2 shows the EPR spectra of a peptide corresponding to the PrP octarepeat domain, PrP(57–91), complexed with copper, as a function of pH. As indicated by the hyperfine splittings, both $g_\parallel$ and $A_\parallel$ shift with increasing pH. This is attributable to a progressive transition from 4O coordination at low pH to 4N coordination at high pH (52,53). There are several archetypal copper centers readily identified by their EPR spectra. Type 1 centers involve sulfur coordination, as found in blue copper proteins, and are characterized by low $A_\parallel$ values, typically

around 50 G. Type 2 centers give spectra similar to those in Figure 1, and they arise from nitrogen and oxygen coordination and have larger $A_{\|}$ values in excess of 150 G (54).

^{14}N has a nuclear spin of $I = 1$ and, when coordinated to copper, often reveals additional superhyperfine couplings. Such couplings are small and typically on the order of 10–15 G. In some cases, these couplings are observable in the intense perpendicular region of the EPR spectrum between 3200 and 3400 G. Under ideal circumstances, the superhyperfine multiplets reflect the number of coordinated nitrogens, with a single nitrogen giving a three-line multiplet, two nitrogens giving a five-line multiplet, and so on. However, if $A_{xx} \neq A_{yy}$, the perpendicular region exhibits overlapping superhyperfine features, thus obscuring detailed couplings.

Superhyperfine interactions are best obtained from the parallel region of the Cu^{2+} spectrum. Unfortunately, inhomogeneous broadening owing to random variations in the coordination environments gives rise to distributions of $g_{\|}$ and $A_{\|}$ values, which are termed *g* strain and *A* strain, respectively, in turn masking subtle spectral features. Froncisz and Hyde (55) recognized, however, that for certain ^{63}Cu hyperfine lines, $g_{\|}$ and $A_{\|}$ shift in opposite directions from systematic changes in the ligand field. Moreover, they reasoned that because $g_{\|}$ depends on magnetic field, and $A_{\|}$ does not, proper selection of magnetic field leads to a mutual cancellation of the *g* and *A* strain, thus revealing the desired superhyperfine interactions. This is achieved for the $m_I = -\frac{1}{2}$ hyperfine line at low S-band spectrometer frequencies (56). Figure 3 shows an example of an S-band EPR spectrum obtained at 3.4 GHz. Expansion of the $m_I = -\frac{1}{2}$ hyperfine line reveals subtle splittings indicative of a multiplet structure arising from coordinated ^{14}N. The seven-line pattern, with a separation of approximately 10 G, suggests that three, or perhaps four, nitrogens are directly coordinated to the copper center. As shown below, selective ^{15}N labeling in conjunction with S-band EPR directly identifies nitrogens coordinated to the Cu^{2+} center.

Electron spin echo–envelope modulation (ESEEM), a pulsed EPR technique, is particularly useful for copper centers. If a copper center is magnetically coupled to a ^{14}N nucleus with a hyperfine energy approximately equal to the nuclear Zeeman energy, the height of a spin echo from a two- or three-pulse sequence exhibits modulations as a function of timing between the pulses (57–59). Near this so-called exact cancellation condition, the frequencies of these modulations, as revealed by Fourier transform, correspond to the energies of the pure ^{14}N quadrupolar transitions. In such cases, ESEEM actually reveals ^{14}N NMR-like transitions, but they are detected by EPR (57–59).

ESEEM is marvelously diagnostic for identifying imidazole coordination to copper arising from histidine (His) side chains. The remote, noncoordinated nitrogen is just the right distance from the copper center to satisfy the exact cancellation condition and maximize the ESEEM signal; Figure 4 shows a characteristic spectrum. The three sharp lines below 2.0 MHz result from transitions among the three nuclear-spin states of the ^{14}N. The broad feature at approximately 4.0 MHz is called the double quantum, or $\Delta m = 2$, transition, the intensity of which often reflects the number of coordinated imidazoles (60).

Structural Features and Affinities of the PrP Cu^{2+} Sites

Previous investigations suggest that copper sites are localized to the octarepeat domain (24–26,28).To identify the specific residues, we examined the octarepeat peptide PrP(23–28, 57–91), where residues 57–91 encompass the octarepeat domain, and the segment 23–28 is included to improve solubility (52). Titration experiments demonstrated that the octarepeat domain takes up four equivalents of copper, in which each exists in a coordination environment comprising approximately three nitrogen atoms and one oxygen atom. By scanning a broad

series of octarepeat peptides with EPR, we further showed that the residues HGGGW in each repeat constitute the fundamental Cu^{2+}-binding unit. Imidazole coordination was unambiguously identified through ESEEM.

To further localize the coordinating atoms, we prepared a library of site specifically ^{15}N-labeled $I=\frac{1}{2}$ octarepeat peptides, enabling us to identify nitrogens through superhyperfine couplings (43). With S-band EPR, a change from ^{14}N to ^{15}N alters the superhyperfine multiplets in the Cu^{2+} $m_I=-\frac{1}{2}$ hyperfine line only for directly coordinated nitrogen atoms. Examination of the spectra in Figure 5 shows that the two glycine (Gly) residues following the His, in each octarepeat segment, coordinate through their amide nitrogens. Using Raman spectroscopy, Miura et al. (61) also identified amide-nitrogen coordination, although their modeling studies suggested the involvement of the second and third Gly residues following the His.

Although the ESEEM spectra of the octarepeat domain clearly identify coordination from the His side chains, there are additional features beyond those expected from a single imidazole group (Figure 4). Using the library of ^{15}N-labeled octarepeat peptides, we showed that the additional features are from the ^{14}N of the third Gly following each His (43). This particular nitrogen is not coordinated to the Cu^{2+} center and, alternatively, is approximately 4.0 Å away, appropriate for a strong ESEEM signal.

Figure 6 shows the Cu^{2+}-coordination environment, based on EPR experiments, along with a crystal structure of the Cu^{2+}-HGGGW complex (43). There is complete agreement between the EPR-defined contacts and the crystal structure. Computational (62) and NMR studies (63) provide further support for this type of coordination environment. Moreover, experiments on selectively labeled PrP(23–28, 57–91) proved that the coordination environment in Figure 6 is preserved in the full octarepeat domain (43). Using full-length recombinant PrP, we also found a nonoctarepeat site involving His-96 (64). The location of this particular site has been controversial, with Jones et al. (65) arguing that Cu^{2+} coordinates at His-111 with higher affinity than at His-96. Figure 7 shows our model of full-length PrP, with all copper sites occupied.

The experiments above were performed on fully Cu^{2+} -occupied octarepeat complexes and thus do not address the details of how PrP responds to intermediate copper concentrations. If each HGGGW copper-binding module sequentially takes up a single equivalent, EPR spectra should be invariant as a function of Cu^{2+} occupancy. Instead, our EPR experiments showed that spectral features vary significantly as a function of copper load, demonstrating an unambiguous rearrangement of the octarepeat domain. Using a series of designed peptides and the EPR methodologies above, we identified three distinct binding components (Figure 8) (66). At low-Cu^{2+} occupancy, which gives rise to the component 3 spectrum, a single Cu^{2+} coordinates through multiple His side chains; at high occupancy, the component 1 spectrum dominates and reflects the interaction with a single His and deprotonated amide side chains, as described in the sections above. Component 2 is an intermediate state in which each Cu^{2+} is coordinated by two His residues, thus forming large intervening loops. Consistent with our findings, potentiometric titrations identify distinct deprotonated binding states depending on the ratio of copper to octarepeat (67). X-ray absorption spectra (68), molecular-modeling studies (69), and NMR-lineshape-broadening experiments (70) also find evidence of multiple His coordination at intermediate Cu^{2+} concentrations.

Assessing PrP's copper-binding affinity and cooperativity has proven to be a thorny issue. Clearly, an accurate assessment of these properties is essential for corroborating potential function. For an enzyme, one expects high affinity (low-dissociation constant), whereas

buffering or sensing functions require a lower affinity matched to the concentration of extracellular copper. Current estimates place the dissociation constant between 10^{-6} M (29, 71) and 10^{-14} M (69), a lack of agreement spanning eight orders of magnitude! There are also reports of highly positive binding cooperativity, in which the affinity ramps up with the addition of each Cu^{2+} (24,29,72). However, the molecular mechanism by which this might take place has not been identified.

Previous measurements of PrP's affinity for Cu^{2+} did not take into account the distinct binding modes, no doubt contributing to the disagreement among the published values. EPR methodologies allow us to perform binding measurements on each of the well-defined coordination modes. Using spectral decomposition, we determined the concentrations of all species as a function of Cu^{2+} concentration (Figure 9) (72a). Next, using peptide constructs designed to favor specific binding modes, we determined the precise affinity for each. At low-copper occupancy, which favors multiple His coordination, the octarepeat domain binds Cu^{2+} with a dissociation constant (K_d) of 0.12 nM.

In contrast, high-copper occupancy, involving coordination through deprotonated amide nitrogens, exhibits a weaker affinity characterized by a K_d in the range 7.0 μM to 12.0 μM. The decrease in affinity (increase in K_d) is consistent with negative cooperativity and a Hill coefficient (at half maximum binding) of approximately 0.7 (72a). The concentration distribution in Figure 9, showing significant populations of intermediates, provides further evidence of negative cooperativity because positive cooperativity suppresses intermediates and favors an equilibrium dominated by the fully unbound and fully bound species. Taken together, these findings demonstrate that PrP responds to an exceptionally wide range of copper concentrations, covering approximately five orders of magnitude.

Insights into PrP Function

PrP's nanomolar Cu^{2+} affinity and localization in synaptic regions have lead to the suggestion that the protein is a neuronal metalloenzyme with SOD activity (40,73,74). However, direct assays of SOD activity have been inconsistent with some measurements identifying weak dismutase function (73) and others finding no activity whatsoever (41,42). Known SODs usually coordinate Cu^{2+} through His side chains in a tetrahedral environment, thus facilitating redox activity between the Cu^{+} and Cu^{2+} states. There are several aspects of the copper-coordination features identified by our experiments that are inconsistent with known SODs. First, the variable structures within the octarepeat domain (Figure 8), which depend on copper concentration, are certainly not characteristic of a well-defined metal-ion-coordination site typically required for catalysis. Moreover, even the highest affinity determined from our measurements is significantly less than that found for copper-dependent SODs, which bind with K_d values on the order of 10^{-14} M. Finally, the strong ligand field provided by the negatively charged amide nitrogens, in the dominant component 1–coordination mode, preferentially stabilizes the Cu^{2+}-oxidation state, and direct electrochemical measurements have confirmed this (75).

PrP protects neurons against oxidative stress from reactive oxygen species or redox active metal ions. For example, it is well established that weakly complexed copper in the micromolar range is toxic to neurons, and cells expressing PrP are much more resistant to this oxidative stress than PrP knockouts (38). Yet, as noted above, there is significant copper efflux at synapses as a consequence of neuronal activity, and the peak synaptic concentrations are likely to exceed 10 μM. We believe that our results point toward an antioxidant function, as opposed to enzymatic function, in which PrP binds extracellular Cu^{2+}, thus quenching copper's intrinsic redox activity (66). Our structural studies show that component 1 is dominant at high occupancy and thus maximizes PrP's antioxidant character at elevated Cu^{2+} concentrations. With these

chemical and structural considerations, PrP's localization at synapses may be part of a protective mechanism in which copper sequestration ameliorates deleterious redox activity during synaptic depolarization. PrP may also play a role in trafficking copper back to the cell interior.

The protein composition of the cerebrospinal fluid in the CNS also points toward a copper-sequestering role for PrP. In the blood and blood plasma, exchangeable copper is bound to a number of molecular species, including amino acids, but the primary copper-buffering component is serum albumin, which takes up one equivalent of Cu^{2+} at its N terminus (76, 77). The concentration of albumin is approximately 600 μM, and its copper-coordination mode stabilizes Cu^{2+}, much like the component 1 complex in PrP. Interestingly, cerebrospinal fluid also contains amino acids but lacks high concentrations of albumin and other copper-binding proteins normally found in blood. Consequently, membrane-bound PrP may, in part, play an albumin-like role, thus helping to maintain copper homeostasis.

Consideration of PrP's octarepeat domain sequence provides further insight into relevant Cu^{2+}-binding modes. Within the octarepeat domain, component 1 coordination requires the residues HGGGW. His anchors Cu^{2+}, and the torsional flexibility of the Gly residues allows for the planar equatorial configuration observed in Figure 6. Garnett & Viles (72) have shown that the replacement of Gly with chiral amino acids such as alanine (Ala) results in an alteration of the copper-coordination environment. Interestingly, in the HGGGW sequence, the His, Gly, and tryptophan (Trp) residues that make direct contact with Cu^{2+} are absolutely conserved in all mammalian sequences (20). The only variability is at the noncoordinating third Gly, where some species, such as mouse, have a Ser in two of the four repeats.

Component 3 coordination, conversely, depends not on the precise details of each octarepeat, but on the number of octarepeats, because each provides a single His; octapeptide sequences with less than three repeats fail to exhibit the component 3–binding mode. Here again, there is absolute sequence conservation among the mammalian sequences with all species possessing four or five repeats (20). These sequence-based observations suggest that the capacity for both component 1– and component 3–coordination modes have been preserved through evolution and are likely involved in PrP function (with component 2 serving as an intermediate). As the discussion above suggests, if component 1 is critical for suppressing Cu^{2+}-redox activity, the role of component 3 may be to confer negative cooperativity, thereby spreading out PrP's response to varying copper concentrations.

Alternatively, the transition among binding modes may serve as a copper-dependent switch that facilitates specific cellular processes. For example, copper concentrations in excess of 100 μM stimulate PrP endocytosis (30); the transition from component 3 to component 1 coordination may be the trigger for this process. Although there is doubt as to whether copper bound to PrP is trafficked by endocytosis, Takeuchi and colleagues (47) recently suggested that, once in the endosome, component 3 coordination facilitates reduction to Cu^{+} as part of copper transport to the intracellular space.

Programmed cell death, termed apoptosis, is an essential process for regulating the number of cells in an organ. Several recent studies show that PrP is antiapoptotic (46,78–80); it protects cells from signals that would otherwise trigger apoptosis. For example, PrP protects against the cellular death brought on by the expression of the Doppel protein (a homolog of C-terminal PrP) (78) or from serum deprivation (80). Mutagenesis experiments show that the PrP octarepeat domain is required for protection against Doppel-protein toxicity (78).

Investigations into the X-linked inhibitor of apoptosis (XIAP), an intracellular protein that negatively regulates apoptotic enzymes, recently identified an intimate link between copper homeostasis and the regulation of cell death (81). Specifically, intracellular copper binds

directly to XIAP, causing a conformational change that accelerates its degradation, thus promoting apoptosis. The authors of this study argued that the build up of copper in Wilson's disease, for example, might upregulate apoptosis, resulting in tissue and organ damage. Thus, copper toxicity may occur through two primary mechanisms: its inherent redox activity and a lowering of the apoptosis threshold. In turn, PrP's antiapoptotic function may arise from its ability to sense copper at the extracellular-membrane surface or to regulate the transmembrane movement of copper.

Copper and PrP^{Sc}

Experiments into the connection between copper and PrP^{Sc} formation reveal contradictory results. It is simply not known whether copper promotes or inhibits prion disease. For example, the copper-binding octarepeats are not necessary for propagating prion infection (82), yet humans with octarepeat expansions are prone to inherited CJD (83). Copper treatment of extracted PrP^{C} converts the protein to a protease-resistant form, perhaps an intermediate en route to PrP^{Sc} (84). Conversely, the addition of copper to protocols used for creating synthetic prions greatly slows amyloid formation, suggesting that copper inhibits PrP^{Sc} (85). In scrapie-infected cellular preparations, the addition of copper reduces the accumulation of PrP^{Sc} (86), yet copper is found in PrP^{Sc} deposits (87), and the removal of copper by chelation seems to delay the onset of prion disease (88).

Several aspects of copper binding likely help explain these divergent results. First, the copper site involving His-96 is in the region of PrP that typically remains after proteolytic cleavage, liberating amyloidogenic, C-terminal PrP^{Sc}. Thus, copper may modulate PrP^{Sc} formation even in the absence of the octarepeats, as Cox et al. (89) recently suggested. Another critical issue, discussed above, is that PrP^{C} binds copper with several unique coordination modes (66). It is certainly possible that each mode exhibits distinct characteristics with regard to prion conversion.

The TSEs are often considered amyloid diseases in which ordered fibrils are a required component of the prion lesions. However, this is not strictly correct. There are many instances of prion diseases, such as certain types of CJD, in which accumulated PrP^{Sc} is devoid of the fibrillar structure of amyloid (21). Moreover, transgenic mice engineered to produce PrP^{C} without the glycosylphosphatidylinositol-membrane anchor, exhibit widespread amyloid accumulation when infected with PrP^{Sc}, but without the usual, profound spongiform degeneration (90).

Prion specialists have long suspected that, in addition to amyloid, small PrP^{Sc} oligomers likely contribute to neuron deterioration. Interestingly, new avenues into the mechanism of neurodegeneration in Alzheimer's disease also focus on prefibrillar aggregates of the Aβ peptide, as opposed to high-molecular-weight fibrils (91,92). Another aspect of these diseases under current consideration is that loss of function of the normal endogenous peptide or protein creates cell stress that contributes to neuronal death (93). In support of this, PrP^{Sc} added to cellular preparations inhibits copper binding to endogenous PrP^{C}, thus rendering cells susceptible to copper toxicity (94). Moreover, cross-linking PrP^{C} with monoclonal antibodies triggers rapid neuronal apoptosis (79). If PrP^{C} protects neuronal integrity, perhaps by suppressing apoptosis, loss of this function may leave cells susceptible to stress, thus contributing to neurodegeneration. As such, the link between PrP and copper is certain to not only elucidate PrP^{C} function, but also to provide important new concepts in the development of neurodegenerative disease.

Summary Points

1. The prion protein (PrP), responsible for the TSEs, is a copper-binding protein of unknown function. In its normal cellular form, PrP^C, the protein acts as a neuroprotectant, thereby maintaining the integrity of cells in the CNS. The protein may function as a SOD, a copper transporter, a copper reductase, or a copper scavenger.
2. Most of the copper ions bind in a domain composed of tandem PHGGGWGQ repeats. At low-Cu^{2+} occupancy, equatorial coordination is provided by three or four His imidazoles; at high occupancy, equatorial coordination is from the His imidazole and deprotonated amide-nitrogen atoms from the two Gly residues that immediately follow His. The high-occupancy coordination mode stabilizes Cu^{2+} over Cu^{+} and thus suppresses copper-redox activity.
3. The affinity for Cu^{2+} varies significantly with K_d values of 0.12 nM at low occupancy and 7–10 μM at high occupancy. Such affinities are well matched to the known Cu^{2+} concentrations in the synapse where PrP is localized.
4. Although there is good evidence that PrP may function as a copper scavenger, much like albumin in the blood, we believe that the protein may also be involved in modulating signals for apoptosis by regulating membrane-surface-bound Cu^{2+}.
5. Copper may also play a role in disease, although it is currently not clear whether the interaction between PrP and Cu^{2+} facilitates or inhibits prion formation. Recent evidence suggests that a loss of normal PrP^C function may contribute to cell stress, thus enhancing neurodegeneration.

Acknowledgments

This work was supported by NIH grant GM065790 and NSF instrumentation grant DBI-0217922. I also thank Dr. Madhuri Chattopadhyay, Dr. Eric Walter, and Ms. Mira Patel for discussion and editorial comments on the manuscript.

Literature Cited

1. Prusiner SB. Molecular biology of prion diseases. Science 1991;252:1515–22. [PubMed: 1675487]
2. Prusiner SB. Prion diseases and the BSE crisis. Science 1997;278:245–51. [PubMed: 9323196]
3. Prusiner SB. Prions. Proc Natl Acad Sci USA 1998;95:13363–83. [PubMed: 9811807]
4. Weissmann C. The state of the prion. Nat Rev Microbiol 2004;2:861–71. [PubMed: 15494743]
5. Prusiner, SB. Prion Biology and Diseases. Cold Spring Harbor, NY: Cold Spring Harbor Lab. Press; 2003. p. 800
6. Lansbury PTJ. Structural neurology: Are seeds at the root of neuronal degeneration? Neuron 1997;19:1151–54. [PubMed: 9427238]
7. Pauli G. Tissue safety in view of CJD and variant CJD. Cell Tissue Bank 2005;6:191–200. [PubMed: 16151959]
8. Miller MW, Williams ES, McCarty CW, Spraker TR, Kreeger TJ, et al. Epizootiology of chronic wasting disease in free-ranging cervids in Colorado and Wyoming. J Wildl Dis 2000;36:676–90. [PubMed: 11085429]
9. Horby P. Variant Creutzfeldt-Jakob disease: an unfolding epidemic of misfolded proteins. J Paediatr Child Health 2002;38:539–42. [PubMed: 12410862]
10. Ironside JW. The spectrum of safety: variant Creutzfeldt-Jakob disease in the United Kingdom. Semin Hematol 2003;40:16–22. [PubMed: 14690064]
11. Ironside JW, Head MW. Variant Creutzfeldt-Jakob disease: risk of transmission by blood and blood products. Haemophilia 2004;10(Suppl. 4):64–69. [PubMed: 15479374]

12. Flechsig E, Weissmann C. The role of PrP in health and disease. Curr Mol Med 2004;4:337–53. [PubMed: 15354865]
13. Zahn R, Liu A, Luhrs T, Riek R, von Schroetter C, et al. NMR solution structure of the human prion protein. Proc Natl Acad Sci USA 2000;97:145–50. [PubMed: 10618385]
14. James TL, Liu H, Nikolai BU, Farr-Jones S, Zhang H, et al. Solution structure of a 142-residue recombinant prion protein corresponding to the infectious fragment of the scrapie isoform. Proc Natl Acad Sci USA 1997;94:10086–91. [PubMed: 9294167]
15. Riek R, Hornemann S, Wider G, Billeter M, Glockshuber R, Wuthrich K. NMR structure of the mouse prion protein domain PrP(121–321). Nature 1996;382:180–82. [PubMed: 8700211]
16. Riek R, Hornemann S, Wider G, Glockshuber R, Wuthrich K. NMR characterization of the full-length recombinant murine prion protein, mPrP(23–231). FEBS Lett 1997;413:282–88. [PubMed: 9280298]
17. Govaerts C, Wille H, Prusiner SB, Cohen FE. Evidence for assembly of prions with left-handed β-helices into trimers. Proc Natl Acad Sci USA 2004;101:8342–47. [PubMed: 15155909]
18. Wille H, Michelitsch MD, Guenebaut V, Supattapone S, Serban A, et al. Structural studies of the scrapie prion protein by electron crystallography. Proc Natl Acad Sci USA 2002;99:3563–68. [PubMed: 11891310]
19. Donne DG, Viles JH, Groth D, Mehlhorn I, James TL, et al. Structure of the recombinant full-length hamster prion protein PrP(29–231): The N-terminus is highly flexible. Proc Natl Acad Sci USA 1997;94:13452–56. [PubMed: 9391046]
20. Wopfner F, Weidenhofer G, Schneider R, von Brunn A, Gilch S, et al. Analysis of 27 mammalian and 9 avian PrPs reveals high conservation of flexible regions of the prion protein. J Mol Biol 1999;289:1163–78. [PubMed: 10373359]
21. Prusiner SB. Shattuck lecture: neurodegenerative diseases and prions. N Engl J Med 2001;344:1516–26. [PubMed: 11357156]
22. Prusiner SB, Groth D, Serban A, Stahl N, Gabizon R. Attempts to restore scrapie prion infectivity after exposure to protein denaturants. Proc Natl Acad Sci USA 1993;90:2793–97. [PubMed: 8464892]
23. Legname G, Baskakov IV, Nguyen HO, Riesner D, Cohen FE, et al. Synthetic mammalian prions. Science 2004;305:673–76. [PubMed: 15286374]
24. Brown DR, Qin K, Herms JW, Madlung A, Manson J, et al. The cellular prion protein binds copper in vivo. Nature 1997;390:684–87. [PubMed: 9414160] This seminal report was the first to draw a convincing connection between PrP and in vivo copper.
25. Hornshaw MP, McDermott JR, Candy JM. Copper binding to the n-terminal tandem repeat regions of mammalian and avian prion protein. Biochem Biophys Res Comm 1995;207:621–29. [PubMed: 7864852]
26. Hornshaw MP, McDermott JR, Candy JM, Lakey JH. Copper binding to the N-terminal tandem repeat region of mammalian and avian prion protein: structural studies using synthetic peptides. Biochem Biophys Res Commun 1995;214:993–99. [PubMed: 7575574]
27. Stöckel J, Safar J, Wallace AC, Cohen FE, Prusiner SB. Prion protein selectively binds copper(II) ions. Biochemistry 1998;37:7185–93. [PubMed: 9585530]
28. Viles JH, Cohen FE, Prusiner SB, Goodin DB, Wright PE, Dyson HJ. Copper binding to the prion protein: structural implications of four identical cooperative binding sites. Proc Natl Acad Sci USA 1999;96:2042–47. [PubMed: 10051591]
29. Whittal RM, Ball HL, Cohen FE, Burlingame AL, Prusiner SB, Baldwin MA. Copper binding to octarepeat peptides of the prion protein monitored by mass spectrometry. Protein Sci 2000;9:332–43. [PubMed: 10716185]
30. Pauly PC, Harris DA. Copper stimulates endocytosis of the prion protein. J Biol Chem 1998;273:33107–19. [PubMed: 9837873]
31. Rachidi W, Vilette D, Guiraud P, Arlotto M, Riondel J, et al. Expression of prion protein increases cellular copper binding and antioxidant enzyme activities but not copper delivery. J Biol Chem 2003;278:9064–72. [PubMed: 12500977]
32. Millhauser GL. Copper binding in the prion protein. Acc Chem Res 2004;37:79–85. [PubMed: 14967054]

33. Herms J, Tings T, Gall S, Madlung A, Giese A, et al. Evidence of presynaptic location and function of the prion protein. J Neurosci 1999;19:8866–75. [PubMed: 10516306]
34. Hartter DE, Barnea A. Evidence for release of copper in the brain: depolarization-induced release of newly taken-up 67copper. Synapse 1988;2:412–15. [PubMed: 3187909]
35. Hopt A, Korte S, Fink H, Panne U, Niessner R, et al. Methods for studying synaptosomal copper release. J Neurosci Methods 2003;128:159–72. [PubMed: 12948559]
36. Kardos J, Kovacs I, Hajos F, Kalman M, Simonyi M. Nerve endings from rat brain tissue release copper upon depolarization: a possible role in regulating neuronal excitability. Neurosci Lett 1989;103:139–44. [PubMed: 2549468]
37. Vassallo N, Herms J. Cellular prion protein function in copper homeostasis and redox signaling at the synapse. J Neurochem 2003;86:538–44. [PubMed: 12859667]
38. Brown DR, Schmidt B, Kretzschmar HA. Effects of copper on survival of prion protein knockout neurons and glia. J Neurochem 1998;70:1686–93. [PubMed: 9523587]
39. Klamt F, Dal-Pizzol F, Conte DA, Frota JML, Walz R, et al. Imbalance of antioxidant defense in mice lacking cellular prion protein. Free Radic Biol Med 2001;30:1137–44. [PubMed: 11369504]
40. Daniels M, Brown DR. Purification and preparation of prion protein: synaptic superoxide dismutase. Methods Enzymol 2002;349:258–67. [PubMed: 11912915]
41. Hutter G, Heppner FL, Aguzzi A. No superoxide dismutase activity of cellular prion protein in vivo. Biol Chem 2003;384:1279–85. [PubMed: 14515989]
42. Jones S, Batchelor M, Bhelt D, Clarke AR, Collinge J, Jackson GS. Recombinant prion protein does not possess SOD-1 activity. Biochem J 2005;392:309–12. [PubMed: 16156720]
43. Burns CS, Aronoff-Spencer E, Dunham CM, Lario P, Avdievich NI, et al. Molecular features of the copper binding sites in the octarepeat domain of the prion protein. Biochemistry 2002;41:3991–4001. [PubMed: 11900542] The first detailed elucidation of the Cu^{2+}-binding features in an octarepeat segment.
44. Waggoner DJ, Drisaldi B, Bartnikas TB, Casareno RLB, Prohaska JR, et al. Brain copper content and cuproenzyme activity do not vary with prion protein expression level. J Biol Chem 2000;275:7455–58. [PubMed: 10713045]
45. Mouillet-Richard S, Ermonval M, Chebassier C, Laplanche JL, Lehmann S, et al. Signal transduction through prion protein. Science 2000;289:1925–28. [PubMed: 10988071]
46. Roucou X, Gains M, LeBlanc AC. Neuroprotective functions of prion protein. J Neurosci Res 2004;75:153–61. [PubMed: 14705136]
47. Miura T, Sasaki S, Toyama A, Takeuchi H. Copper reduction by the octapeptide repeat region of prion protein: pH dependence and implications in cellular copper uptake. Biochemistry 2005;44:8712–20. [PubMed: 15952778]
48. Kanaani J, Prusiner SB, Diacovo J, Baekkeskov S, Legname G. Recombinant prion protein induces rapid polarization and development of synapses in embryonic rat hippocampal neurons in vitro. J Neurochem 2005;95:1373–86. [PubMed: 16313516]
49. Eghiaian F, Grosclaude J, Lesceu S, Debey P, Doublet B, et al. Insight into the PrP^{C}–>PrP^{Sc} conversion from the structures of antibody-bound ovine prion scrapie-susceptibility variants. Proc Natl Acad Sci USA 2004;101:10254–59. [PubMed: 15240887]
50. Haire LF, Whyte SM, Vasisht N, Gill AC, Verma C, et al. The crystal structure of the globular domain of sheep prion protein. J Mol Biol 2004;336:1175–83. [PubMed: 15037077]
51. Peisach J, Blumberg WE. Structural implications derived from the analysis of electron paramagnetic resonance spectra of natural and artificial copper proteins. Arch Biochem Biophys 1974;165:691–708. [PubMed: 4374138]
52. Aronoff-Spencer E, Burns CS, Avdievich NI, Gerfen GJ, Peisach J, et al. Identification of the Cu^{2+} binding sites in the N-terminal domain of the prion protein by EPR and CD spectroscopy. Biochemistry 2000;39:13760–71. [PubMed: 11076515]
53. Van Doorslaer S, Cereghetti GM, Glockshuber R, Schweiger A. Unraveling the Cu^{2+} binding sites in the C-terminal domain of the murine prion protein: a pulse EPR and ENDOR study. J Phys Chem 2001;105:1631–39.
54. Lippard, SJ.; Berg, JM. Principles of Bioinorganic Chemistry. Mill Valley, CA: Univ. Sci. Books; 1994. p. 411

55. Froncisz W, Hyde JS. Broadening by strains of lines in the *g*-parallel region of Cu^{2+} ion EPR spectra. J Phys Chem 1980;73:3123–31.

56. Yuan H, Antholine WE, Kroneck PMH. Complexation of type 2 copper by cytochrome *c* oxidase: probing of metal-specific binding sites by electron paramagnetic resonance. J Inorg Biochem 1998;71:99–107. [PubMed: 9755494]

57. Flanagan HL, Singel DJ. Analysis of ^{14}N ESEEM patterns of randomly oriented solids. J Chem Phys 1987;87:5606–16.

58. Mims WB, Peisach J. The nuclear modulation effect in electron spin echoes for complexes of Cu^{2+} and imidazole with ^{14}N and ^{15}N. J Chem Phys 1978;69:4921–30.

59. Mims, WB.; Peisach, J. Electron spin echo spectroscopy and the study of metalloproteins. In: Berliner, LJ.; Reuben, J., editors. Biological Magnetic Resonance. New York: Plenum; 1981.

60. McCracken J, Pember S, Benkovic SJ, Villafranca JJ, Miller RJ, Peisach J. Electron-spin echo studies of the copper-binding site in phenylalanine-hydroxylase from chromobacterium-violaceum. J Am Chem Soc 1988;110:1069–74.

61. Miura T, Hori-i A, Mototani H, Takeuchi H. Raman spectroscopic study on the copper(II) binding mode of prion octapeptide and its pH dependence. Biochemistry 1999;38:11560–69. [PubMed: 10471308]

62. Pushie MJ, Rauk A. Computational studies of Cu(II)[peptide] binding motifs: Cu[HGGG] and Cu [HG] as models for Cu(II) binding to the prion protein octarepeat region. J Biol Inorg Chem 2003;8:53–65. [PubMed: 12459899]

63. Zahn R. The octapeptide repeats in mammalian prion protein constitute a pH-dependent folding and aggregation site. J Mol Biol 2003;334:477–88. [PubMed: 14623188]

64. Burns CS, Aronoff-Spencer E, Legname G, Prusiner SB, Antholine WE, et al. Copper coordination in the full-length, recombinant prion protein. Biochemistry 2003;42:6794–803. [PubMed: 12779334] Identified copper-binding sites outside of the octarepeat domain.

65. Jones CE, Klewpatinond M, Abdelraheim SR, Brown DR, Viles JH. Probing Cu^{2+} binding to the prion protein using diamagnetic Ni^{2+} and 1H NMR: the unstructured N terminus facilitates the coordination of six Cu^{2+} ions at physiological concentrations. J Mol Biol 2005;346:1393–407. [PubMed: 15713489]

66. Chattopadhyay M, Walter ED, Newell DJ, Jackson PJ, Aronoff-Spencer E, et al. The octarepeat domain of the prion protein binds Cu(II) with three distinct coordination modes at pH7.4. J Am Chem Soc 2005;127:12647–56. [PubMed: 16144413] EPR methodologies show that the molecular features of Cu^{2+} coordination in the octarepeat domain depend on the amount of bound copper.

67. Valensin D, Luczkowski M, Mancini FM, Legowska A, Gaggelli E, et al. The dimeric and tetrameric octarepeat fragments of prion protein behave differently to its monomeric unit. Dalton Trans 2004;2004:284–93.

68. Morante S, Gonzalez-Iglesias R, Potrich C, Meneghini C, Meyer-Klaucke W, et al. Inter- and intraoctarepeat Cu(II) site geometries in the prion protein: implications in Cu(II) binding cooperativity and Cu(II)-mediated assemblies. J Biol Chem 2004;279:11753–59. [PubMed: 14703517]

69. Jackson GS, Murray I, Hosszu LLP, Gibbs N, Waltho JP, et al. Location and properties of metal-binding sites on the human prion protein. Proc Natl Acad Sci USA 2001;98:8531–35. [PubMed: 11438695]

70. Wells MA, Jackson GS, Jones S, Hosszu LL, Craven CJ, et al. A reassessment of copper (II) binding in the full-length prion protein. Biochem J. 2006 In press.

71. Kramer ML, Kratzin HD, Schmidt B, Romer A, Windl O, et al. Prion protein binds copper within the physiological concentration range. J Biol Chem 2001;276:16711–19. [PubMed: 11278306]

72. Garnett AP, Viles JH. Copper binding to the octarepeats of the prion protein. Afffinity, specificity, folding and cooperativity: insights from circular dichroism. J Biol Chem 2003;278:6795–802. [PubMed: 12454014]

72a. Walter ED, Chattopadhyay M, Millhauser GL. The affinity of copper binding to the prion protein octarepeat domain: evidence for negative cooperativity. Biochemistry. 2006 In press.

73. Brown DR, Wong BS, Hafiz F, Clive C, Haswell SJ, Jones IM. Normal prion protein has an activity like that of superoxide dismutase. Biochem J 1999;344:1–5. [PubMed: 10548526]

74. Brown DR. Prion and prejudice: normal protein and the synapse. Trends Neurosci 2001;24:85–90. [PubMed: 11164938]

75. Bonomo RP, Impellizzeri G, Pappalardo G, Rizzarelli E, Tabbi G. Copper(II) binding modes in the prion octarepeat PHGGGWGQ: a spectroscopic and voltammetric study. Chem Eur J 2000;6:4195–202.

76. May PM, Linder PW, Williams DR. Computer simulation of metal-ion equilibria in biofluids: models for the low-molecular-weight complex distribution of calcium(II), magnesium(II), manganese(II), iron(III), copper(II), zinc(II), and lead(II) ions in human blood plasma. J Chem Soc Dalton Trans 1977;1977:588–95.

77. Harford C, Sarkar B. Amino terminal Cu(II)- and Ni(II)-binding (ATCUN) motif of proteins and peptides: metal binding, DNA cleavage, and other properties. Acc Chem Res 1997;30:123–30.

78. Drisaldi B, Coomaraswamy J, Mastrangelo P, Strome B, Yang J, et al. Genetic mapping of activity determinants within cellular prion proteins: N-terminal modules in PrPC offset proapoptotic activity of the Doppel helix B/B′ region. J Biol Chem 2004;279:55443–54. [PubMed: 15459186] These experiments with the doppel protein show that PrP protects against apoptosis, and this activity requires the octarepeat domain.

79. Solforosi L, Criado JR, McGavern DB, Wirz S, Sanchez-Alavez M, et al. Cross-linking cellular prion protein triggers neuronal apoptosis in vivo. Science 2004;303:1514–16. [PubMed: 14752167]

80. Kim BH, Lee HG, Choi JK, Kim JI, Choi EK, et al. The cellular prion protein (PrPC) prevents apoptotic neuronal cell death and mitochondrial dysfunction induced by serum deprivation. Brain Res Mol Brain Res 2004;124:40–50. [PubMed: 15093684]

81. Mufti AR, Burstein E, Csomos RA, Graf PC, Wilkinson JC, et al. XIAP is a copper binding protein deregulated in Wilson's disease and other copper toxicosis disorders. Mol Cell 2006;21:775–85. [PubMed: 16543147]

82. Flechsig, E.; Shmerling, D.; Hegyi, I.; Raeber, AJ.; Fischer, M., et al. Neuron. Vol. 27. 2000. Prion protein devoid of the octapeptide repeat region restores susceptibility to scrapie in PrP knockout mice; p. 399-408.Prion diseases develop more slowly in transgenic animals that express PrP lacking the octarepeats.

83. Goldfarb LG, Brown P, McCombie WR, Goldgaber D, Swergold GD, et al. Transmissible familial Creutzfeldt-Jakob disease associated with five, seven, and eight extra octapeptide coding repeats in the PRNP gene. Proc Natl Acad Sci USA 1991;88:10926–30. [PubMed: 1683708] Humans with octarepeat expansions are susceptible to CJD.

84. Quaglio E, Chiesa R, Harris DA. Copper converts the cellular prion protein into a protease-resistant species that is distinct from the scrapie isoform. J Biol Chem 2001;276:11432–38. [PubMed: 11278539]

85. Bocharova OV, Breydo L, Salnikov VV, Baskakov IV. Copper(II) inhibits in vitro conversion of prion protein into amyloid fibrils. Biochemistry 2005;44:6776–87. [PubMed: 15865423] Copper may slow the formation of infectious prions.

86. Hijazi N, Shaked Y, Rosenmann H, Ben-Hur T, Gabizon R. Copper binding to PrP^C may inhibit prion disease propagation. Brain Res 2003;993:192–200. [PubMed: 14642846]

87. Wadsworth DF, Hill AF, Joiner S, Jackson GS, Clarke AR, Collinge J. Strain-specific prion-protein conformation determined by metal ions. Nat Cell Biol 1999;1:55–59. [PubMed: 10559865]

88. Sigurdsson EM, Brown DR, Alim MA, Scholtzova H, Carp R, et al. Copper chelation delays the onset of prion disease. J Biol Chem 2003;278:46199–202. [PubMed: 14519758]

89. Cox DL, Pan J, Singh RR. Amechanism for copper inhibition of infectious prion conversion. Biophys J 2006;91:L11–13. [PubMed: 16698781]

90. Chesebro B, Trifilo M, Race R, Meade-White K, Teng C, et al. Anchorless prion protein results in infectious amyloid disease without clinical scrapie. Science 2005;308:1435–39. [PubMed: 15933194]

91. Bitan G, Kirkitadze MD, Lomakin A, Vollers SS, Benedek GB, Teplow DB. Amyloid β-protein (Aβ) assembly: Aβ40 and Aβ42 oligomerize through distinct pathways. Proc Natl Acad Sci USA 2003;100:330–35. [PubMed: 12506200]

92. Kayed R, Head E, Thompson JL, McIntire TM, Milton SC, et al. Common structure of soluble amyloid oligomers implies common mechanism of pathogenesis. Science 2003;300:486–89. [PubMed: 12702875]
93. Bush AI. The metallobiology of Alzheimer's disease. Trends Neurosci 2003;26:207–14. [PubMed: 12689772]
94. Rachidi W, Mange A, Senator A, Guiraud P, Riondel J, et al. Prion infection impairs copper binding of cultured cells. J Biol Chem 2003;278:14595–98. [PubMed: 12637548]

Glossary

PrP	prion protein
TSE	transmissible spongiform encephalopathy
CJD	Creutzfeldt-Jakob disease
CNS	central nervous system
PrP^{C}	cellular isoform of PrP
PrP^{Sc}	scrapie isoform of PrP
SOD	superoxide dismutase
EPR	electron paramagnetic resonance
PrP(57–91)	residues 57 through 91 of PrP
K_d	dissociation constant

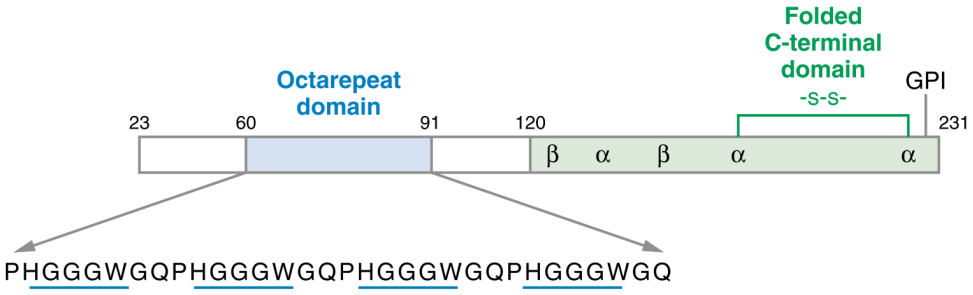

Figure 1.
Diagram indicating secondary structure and other features of the prion protein (PrP). The C-terminal domain contains three α-helical segments, two short β-strands, a disulfide bond, and a glycosylphosphatidylinositol (GPI) anchor that tethers PrP to the membrane surface. The N-terminal segment, up to approximately residue 120, is largely unstructured and contains the octarepeat domain that binds Cu^{2+}.

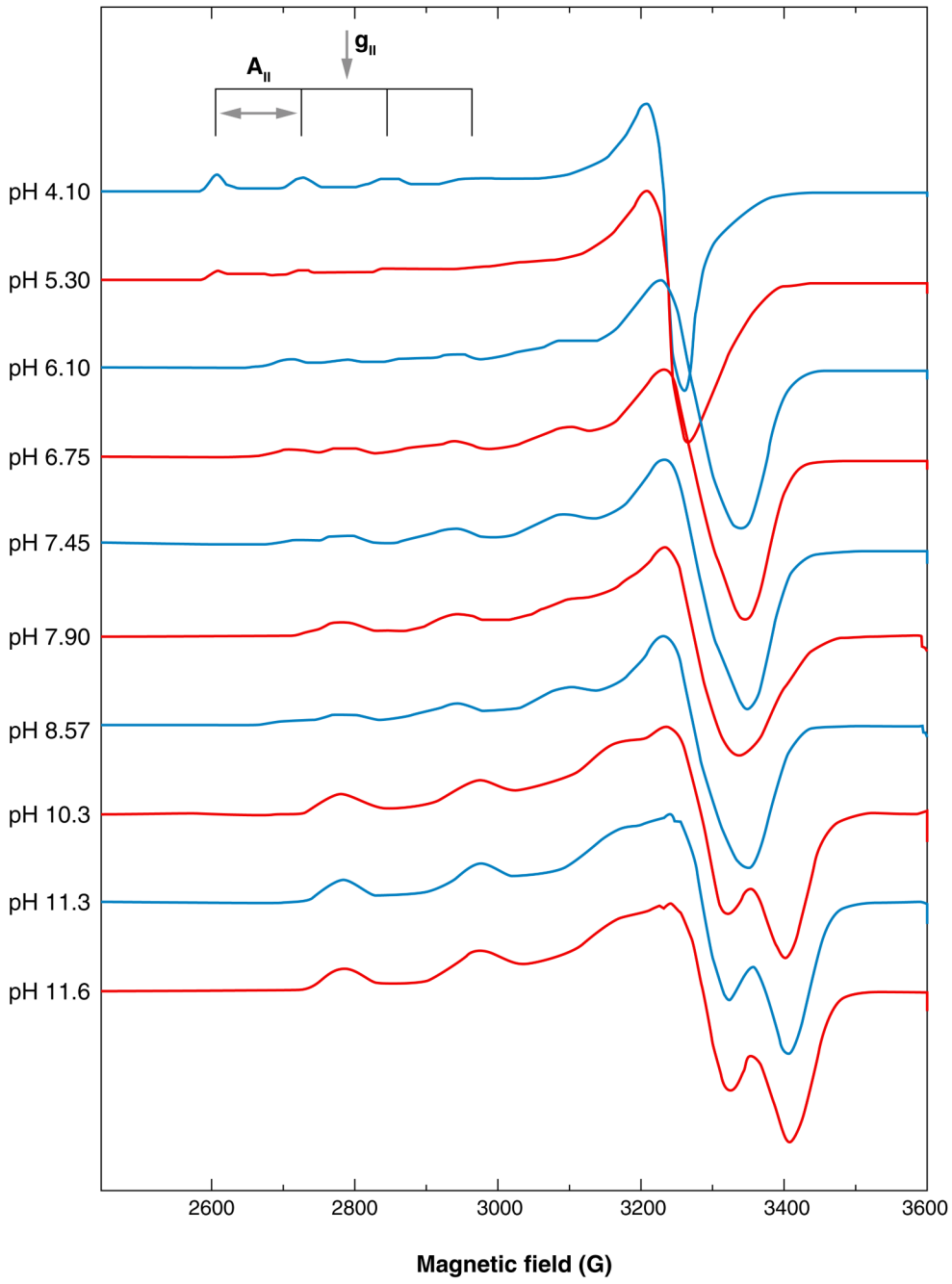

Figure 2.
Electron paramagnetic resonance spectra PrP(57–91) complexed with Cu^{2+}, at 77 K, as a function of pH. Note the systematic changes in $g_{\|}$ and $A_{\|}$.

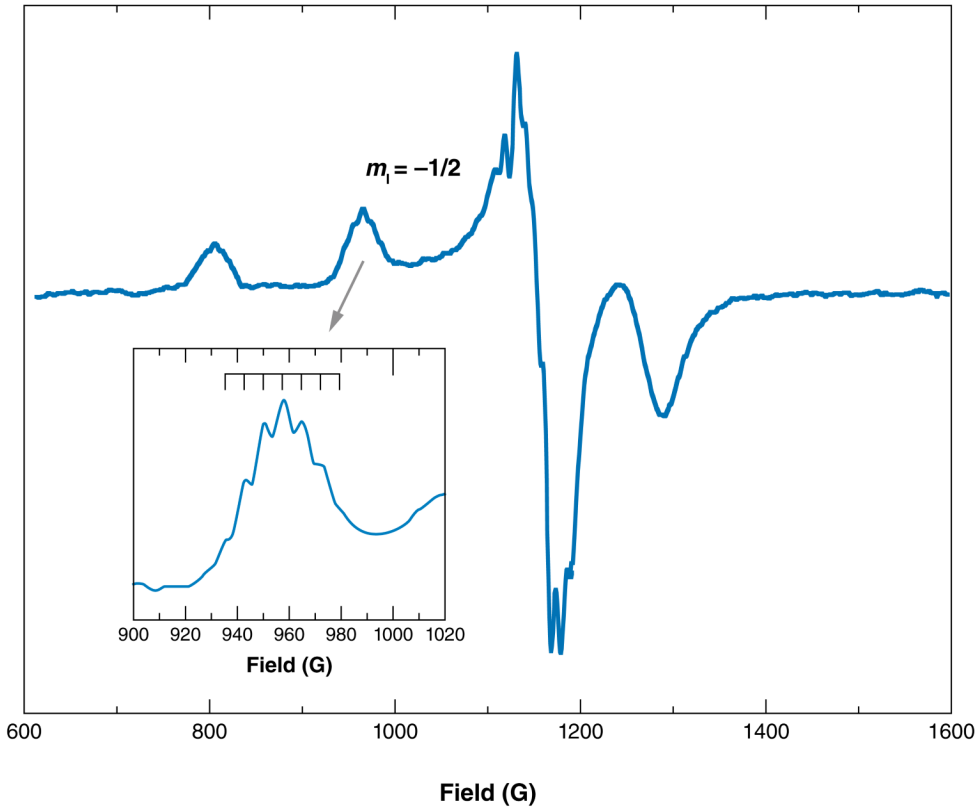

Figure 3.
Low-frequency S-band electron paramagnetic resonance spectrum of a copper center. The $m_I = -\frac{1}{2}$ line is particularly sensitive to nitrogen superhyperfine couplings. The inset shows the expansion of the $m_I = -\frac{1}{2}$ line, revealing seven lines consistent with three ^{14}N atoms in equatorial coordination to the Cu^{2+}.

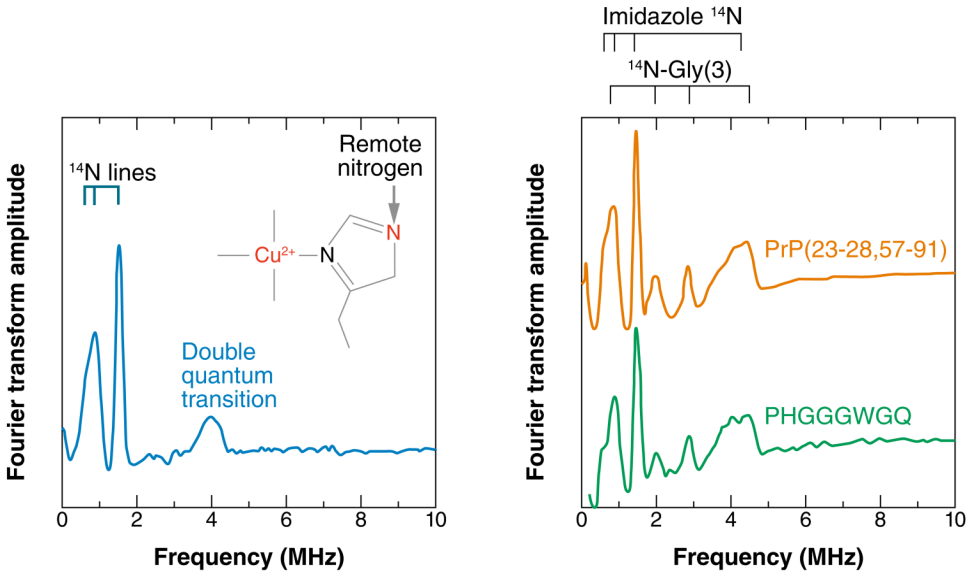

Figure 4.

(*Left panel*) Characteristic electron spin echo–envelope modulation (ESEEM) spectrum of a copper center containing an equatorial imidazole. The observed frequencies arise from the remote nitrogen, as indicated. The lines below 2 MHz arise from transitions among the three ^{14}N nuclear-spin states. The double quantum transition is often enhanced if there is more than one imidazole coordinated to the copper center. (*Right panel*) ESEEM spectra of the octarepeat domain and an individual octarepeat. Equivalence of these spectra shows that the HGGGW coordination mode is preserved in the full domain. The second set of lines arises from the noncoordinated nitrogen from the third glycine (Gly).

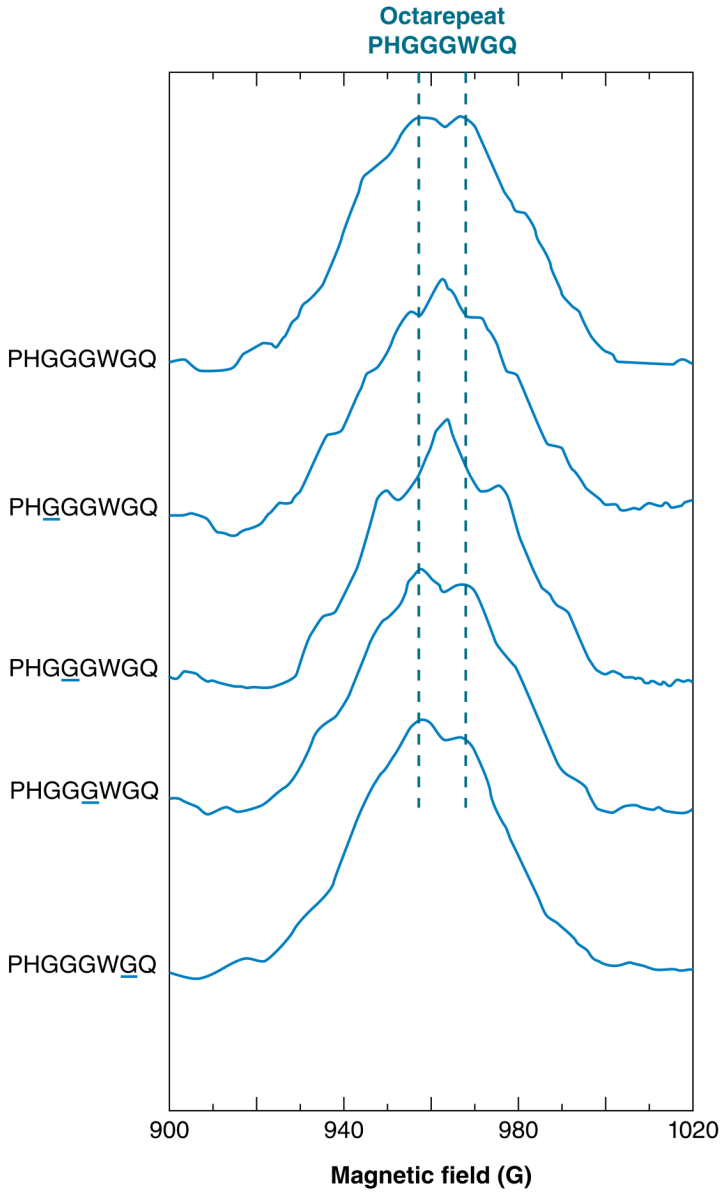

Figure 5.

The $m_I = -\frac{1}{2}$ hyperfine line from the S-band electron paramagnetic resonance spectrum of PHGGGWGQ, with singly ^{15}N-labeled octarepeat peptides (labeled at the underlined residue). The change in multiplet structure arising from labeling at the first and second glycine residues demonstrates that these amino acids coordinate Cu^{2+} through their amide nitrogens.

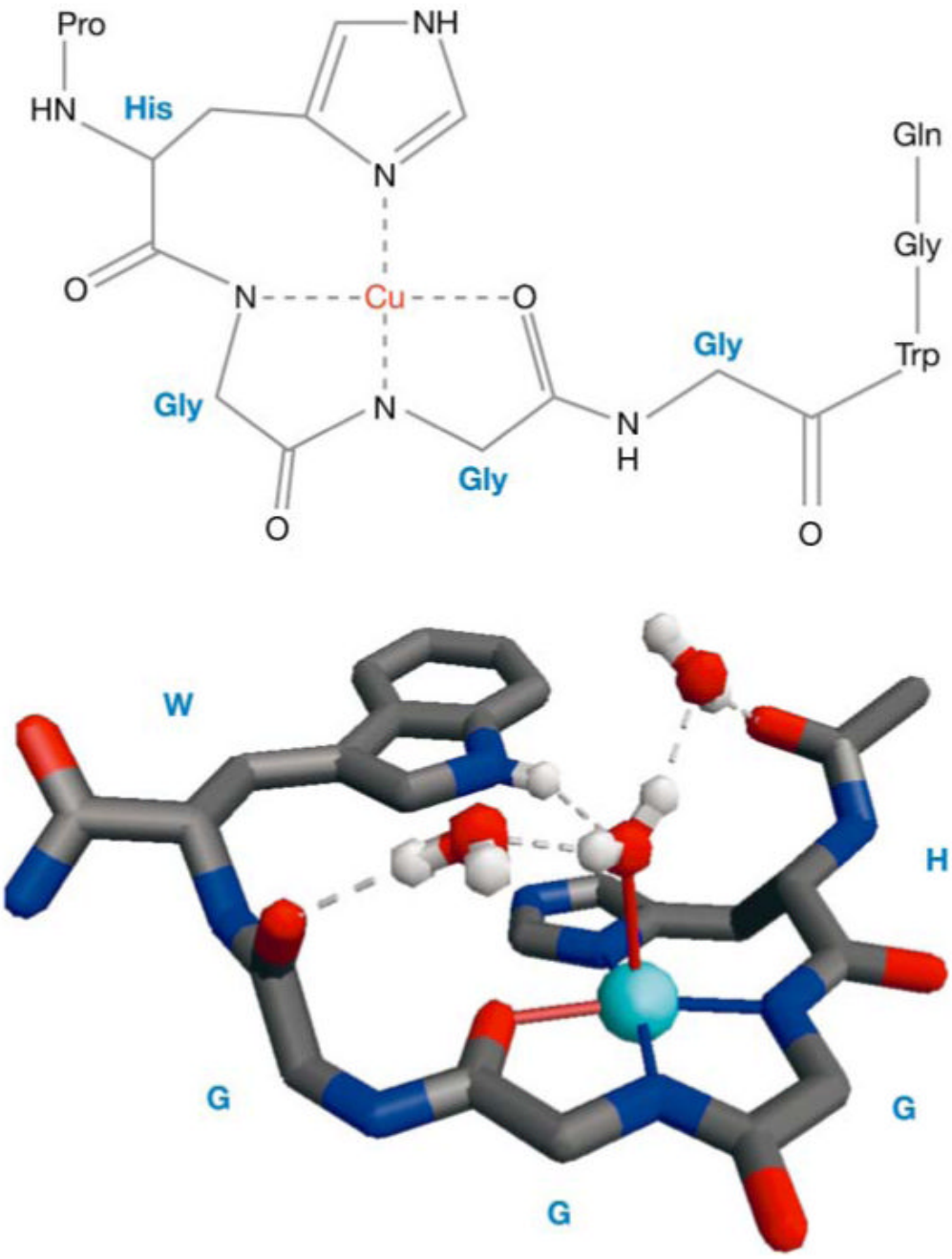

Figure 6.
Chemical details of the Cu^{2+}-octarepeat interaction (*top panel*), determined from electron paramagnetic resonance (EPR) constraints, and the X-ray crystal structure (*bottom panel*) of the Cu^{2+}-HGGGW complex. The molecular features of the crystal structure are fully consistent with the structural details elucidated by EPR. Gly, glycine; His, histidine; Pro, proline; Trp, tryptophan.

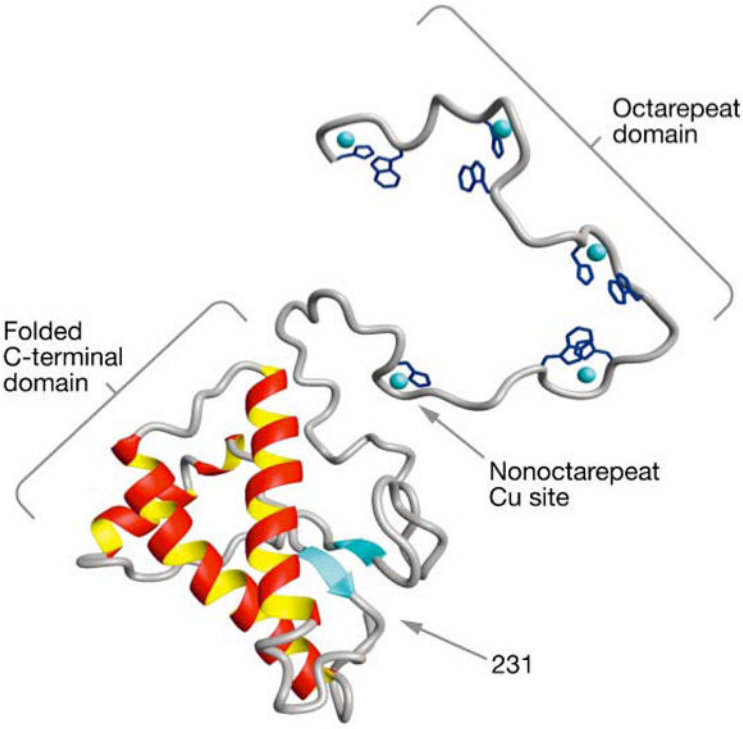

Figure 7.
A structural model of the prion protein with its full complement of copper. Each copper in the octarepeat domain interacts with the HGGGW residues as shown in Figure 6. Electron paramagnetic resonance studies on full-length recombinant protein identified an additional nonoctarepeat binding site involving His-96.

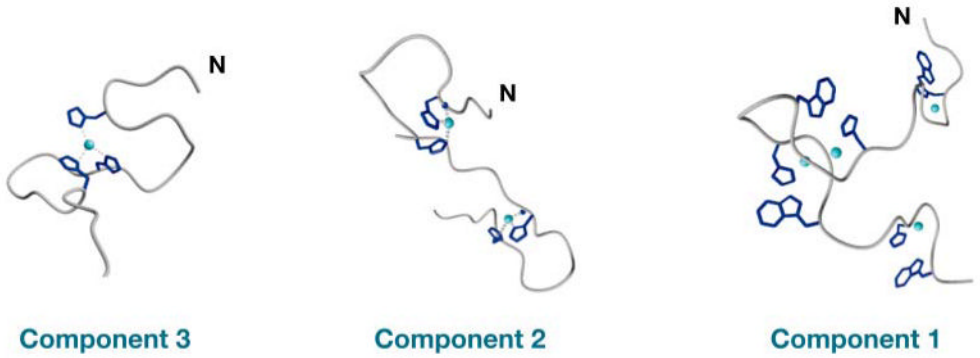

Figure 8.
Distinct octarepeat Cu^{2+} binding modes with three, two, or one coordinated His residues, respectively. Low-Cu^{2+} occupancy favors component 3; high occupancy favors component 1.

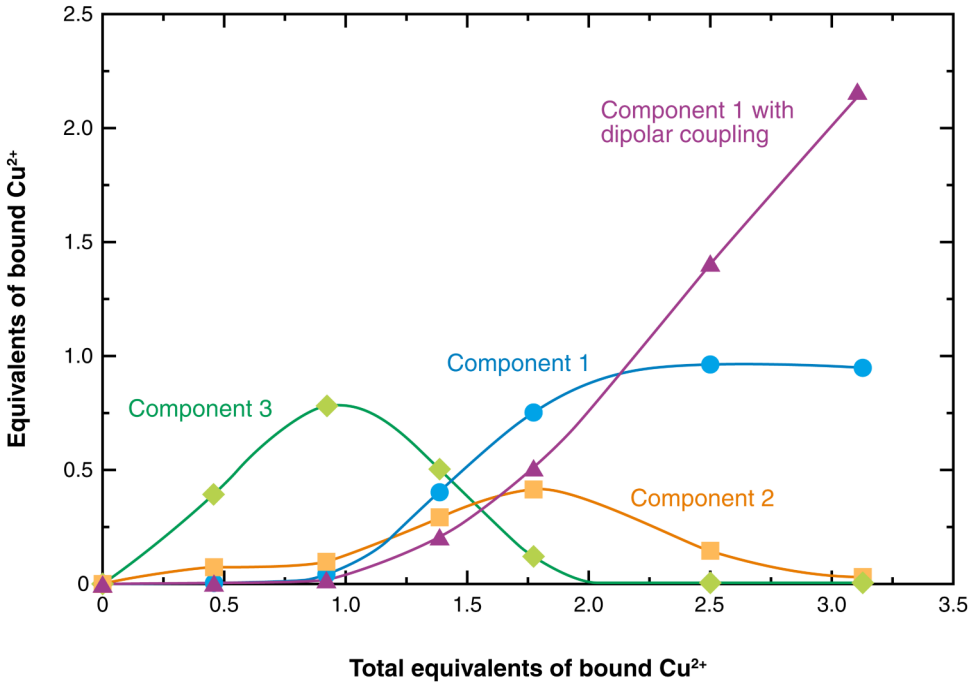

Figure 9.

Relative populations of components 1, 2, and 3 (see Figure 8) as a function of total bound Cu^{2+}. The dipolar-coupled spectrum occurs at full copper occupancy of PrP(23–28, 57–97) and arises from copper-copper couplings between component 1 centers. The significant population of intermediate species, such as component 3, is consistent with negative cooperativity.